SUPPORTING INFORMATION

—

Batch-fabrication of cantilevered magnets on attonewton-sensitivity mechanical oscillators for scanned-probe nanoscale magnetic resonance imaging

Steven A. Hickman,[1] Eric W. Moore,[1] SangGap Lee,[1] Jonilyn G. Longenecker,[1] Sarah J. Wright,[1] Lee E. Harrell,[2] and John A. Marohn[1,*]

[1]*Department of Chemistry and Chemical Biology Cornell University, Ithaca, New York 14853-1301*

[2]*Department of Physics and Nuclear Engineering U.S. Military Academy, West Point, New York 10996*

(Dated: October 14, 2010)

We present cantilever magnetometry data from additional representative cantilevers and, as a control, a blank cantilever. We report surface frequency noise spectra collected at various tip-sample separations.

Cantilever Mechanical Properties

Beyond the cantilever discussed in the manuscript, three additional cantilevers were examined in detail for comparison. See Table I. Cantilever C1 in the table is the cantilever presented in Figures 4, 5, and 8 of the manuscript. Cantilever C2, like C1, has a nickel tip which overhangs the leading edge of the cantilever. Cantilevers C1 and C2 were taken from the same wafer. Cantilever C3's tip magnet does not overhang the leading edge of the cantilever and the magnet is wider and thinner than the magnets on cantilevers C1 and C2. Cantilever C4 has no magnetic tip. Cantilevers C3 and C4 were taken from a second, nominally identical, wafer. Cantilever C5 was fabricated separately from a third wafer; its tip was studied by high resolution electron microscopy to produce Figures 6 and 7 in the manuscript.

Cantilever frequency f_0 was measured as described in the Methods section of the manuscript. Cantilever quality factor Q and spring constant k were inferred as described in the Supplement of Ref.1, by analyzing cantilever ring-down transients and thermomechanical fluctuations,[2] respectively. Comparing cantilevers C1 and C2 to cantilever C3, we see that mechanical quality factor varied significantly from batch to batch (e.g., wafer to wafer). Within one wafer, quality factor showed comparatively less variation. For example, every cantilever examined from the C1 wafer exhibited $Q > 10^5$.

The cantilever Q's in Table I were measured at zero applied magnetic field. In the electron spin resonance experiment described in the manuscript, a magnetic field was applied along the width of cantilever C1. No change in the Q of cantilever C1 was detectable for magnetic fields, up to 1 T, when the field was applied in a direction parallel to the cantilever width.

The cantilever friction coefficient in Table I was calculated from measured cantilever properties using $\Gamma = k/(2\pi f_0 Q)$ and the minimum detectable force was calculated from $F_{\mathrm{min}} = (4k_bT\ \Gamma\ b)^{1/2}$ assuming a temperature of $T = 4.2$. K and a detection bandwidth of $b = 1$ Hz. The force sensitivity of the cantilevers was in the range $3 - 7$ aN. Comparing cantilevers C1 – C3 to C4, we conclude that the presence of the nickel tip has no discernible effect on cantilever sensitivity.

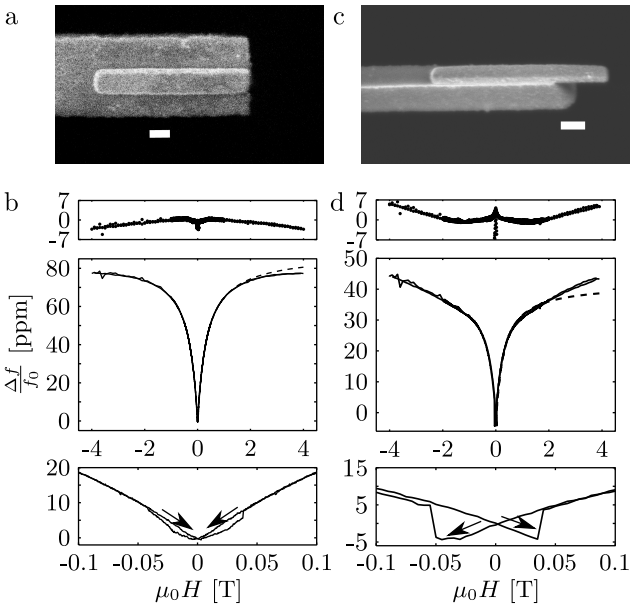

FIG. 1: Characterization of cantilever C2 and C3 tip magnetization. (a) Scanning electron micrograph (SEM) of the leading edge of cantilever C3. The scale bar is 200 nm. (b) Cantilever C3 fractional frequency shift versus magnetic field. (c) SEM of the leading edge of cantilever C2. Note that the magnet overhangs the leading edge of the cantilever by 280 nm. The scale bar is 200 nm. (d) Cantilever C2 fractional frequency shift versus magnetic field.

Cantilever Tip Magnetization

In Fig. 4(a-b) of the manuscript, we presented and analyzed cantilever magnetometry data from cantilever C1. Here we present and analyze cantilever magnetometry data from cantilevers C2 and C3 for comparison.

Scanning electron micrographs of the cantilevers' leading edges can be seen in Fig. 1(a,c). Plots of fractional cantilever frequency shift versus magnetic field, from -4 T to $+4$ T, can be seen in Fig. 1(b,d). In the bottom of Fig. 1(b,d) we plot the fractional cantilever frequency shift from -0.1 T to $+0.1$ T. Both C2 and C3 show clear evidence of frequency

	quantity	C1	C2	C3	C4	C5	unit
cantilever dimensions	l	200	200	200	200	200	μm
	w	4	4	4	4	4	μm
	t	0.34	0.34	0.34	0.34	0.34	μm
cantilever properties at $T = 4.2$ K	f_0	8920	8705	8778	8928	–	Hz
	Q	235 000	189 000	86 500	85 000	–	(unitless)
	k	780 ± 30	870 ± 80	780 ± 130	710 ± 50	–	$\times 10^{-6}$ N m^{-1}
	Γ	59	84	163	149	–	$\times 10^{-15}$ N s m^{-1}
	F_{min}	3.7	4.4	6.2	5.9	–	$\times 10^{-18}$ N
magnet dimensions	l_{m}	1475	1475	1500		1500	nm
	l_{overhang}	350	280	0		420	nm
	w_{m}	111	123	200		150	nm
	t_{m}	100	100	50		100	nm
magnet properties at $T = 4.2$ K	μ_{sat}	5.25 ± 0.79	5.85 ± 0.53	8.04 ± 1.29		–	$\times 10^{-15}$ A m^{-2}
	$\mu_0 M_{\text{sat}}$	0.40 ± 0.07	0.41 ± 0.04	0.68 ± 0.11		–	T
	ΔN	0.69 ± 0.05	0.71 ± 0.07	0.54 ± 0.09		–	(unitless)
note: source wafer		W1	W1	W2	W2	W3	

TABLE I: Summary of the properties of four representative cantilevers at low temperature ($T = 4.2$ K) in high vacuum ($P = 10^{-6}$ mbar). Cantilevers C1, C2, C3, and C5 have an integrated nickel tip; C4 does not. Here l, w, and t are cantilever length, width, and thickness, respectively; f_0, Q, k, and Γ are cantilever resonance frequency, quality factor, spring constant, and friction coefficient, respectively; l_{m}, w_{m}, and t_{m}, are the nickel magnet length, width, and thickness, respectively; l_{overhang} is the magnet "overhang" — the distance that the magnet extends beyond that cantilever's leading edge; and μ_{sat}, $\mu_0 M_{\text{sat}}$, and ΔN are magnet saturation magnetic moment, saturation magnetization, and demagnetization factor difference, respectively. The minimum detectable force F_{min} was calculated assuming a temperature of $T = 4.2$ K and a detection bandwidth of $b = 1$ Hz.

hysteresis near zero field, indicative of a ferromagnetic tip.[3–5] Cantilever C2's tip shows multidomain switching, while cantilever C3's tip is behaving as a single domain magnetic particle with a coercive field of 40 to 50 mT. Cantilever C2 also showed different behavior from C3 at high field. Cantilever C3's frequency was well behaved up to ± 9 T, while C2's frequency showed unexpected but reproducible dips above and below ± 4 T (see Fig. 2).

Analysis of the frequency-shift versus field data indicated that both C2 and C3 were well magnetized. The tip saturation magnetic moment μ_{sat}, saturation magnetization $\mu_0 M_{\text{sat}}$, and demagnetization factor difference ΔN (defined in the manuscript's Method's section) for cantilevers C2 and C3 was obtained by fitting the -4 T to $+4$ T data of Fig. 1(b,d) to Eq. 1 in the manuscript's Methods section.[5] In Fig. 1(b,d), the frequency data is shown as a solid line, the best-fit curve is shown as a dotted line, and the residuals are plotted on top. The results of fitting the data of Fig. 1(b,d) are summarized at the bottom of Table I. The measured magnetic moment of C3's tip was between 94 and 130% of the moment expected given the measured tip volume and nickel's saturation magnetization of $\mu_0 M_{\text{sat}} = 0.6$ T. The measured magnetic moment of C2's tip was between 61 and 74% of the expected total magnetic moment. Prior to fitting the frequency shift versus field data, the baseline response of a bare cantilever (C4) was subtracted away; see Fig. 3.

Electron spin resonance data presented in the manuscript indicated that C1's tip was nevertheless well magnetized at its leading edge; comparing measured to simulated electron spin resonance data suggested the presence of a nonmagnetic layer in the tip's overhanging region whose thickness was 12 nm or less. Consequently, although the magnetometry data indicate that the non-overhanging magnetic tip C3 is fully magnetized while the overhanging tips C1 and C2 are not, we believe that this difference in tip magnetic moment is primarily related to run-to-run variations in the fabrication process and not due to damage incurred during the underetching step required to obtain the overhang. In order to better compare cantilevers, future studies should draw overhanging and non-overhanging magnet-tip cantilevers from the same wafer.

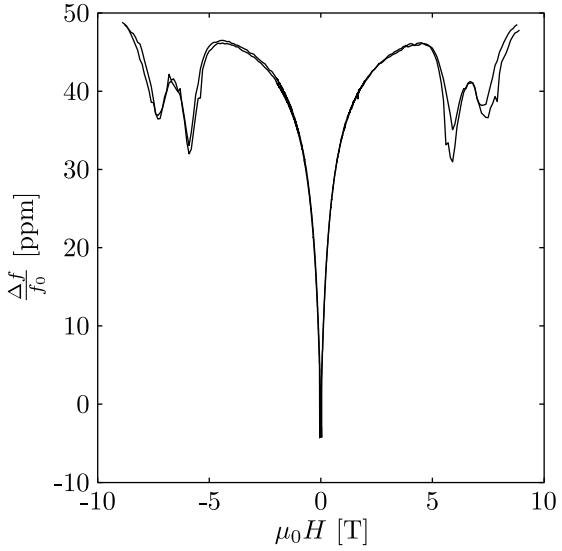

FIG. 2: Cantilever C2 fractional frequency shift versus magnetic field, from -9 T to $+9$ T. Two sweeps are presented.

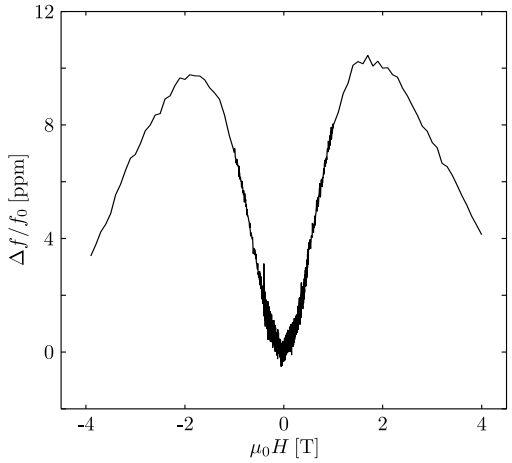

FIG. 3: Fractional frequency shift versus magnetic field of cantilever C4, showing a typical background frequency shift observed with a cantilever having no magnetic tip.

Surface Frequency Noise

Although cantilevers with overhanging tips experienced very little surface force noise (manuscript Fig. 4(e,f)), they experience large surface frequency noise at close tip-sample separations.

In Fig. 4 we plot the power spectral density of cantilever frequency fluctuations versus offset frequency observed over the gold-coated sample described in the manuscript. At each tip-sample separation, the tip-sample voltage was adjusted to give the smallest frequency noise and twenty-five, 25 s transients of cantilever frequency were recorded as described in the manuscript and analyzed as described in the Supplement of Ref.6. Frequency noise power spectra are shown in Fig. 4 for tip-sample separations ranging from $h = 18$ nm to $h = 1$ μm.

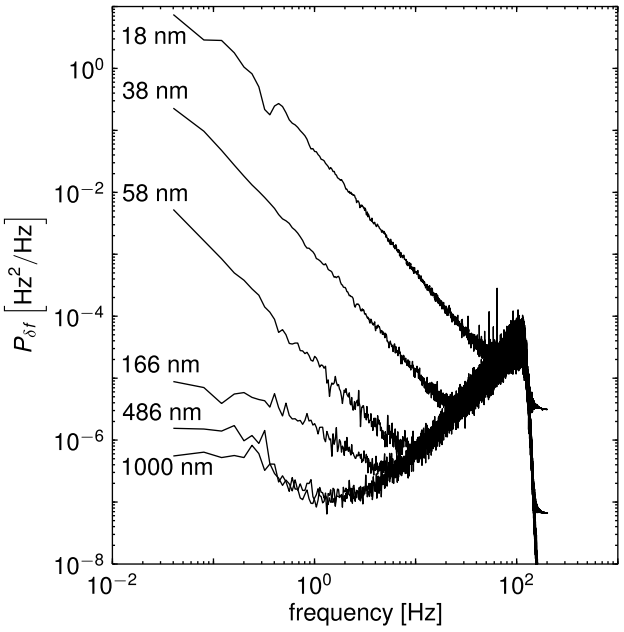

FIG. 4: Cantilever frequency noise power spectra at various tip-sample separations.

At all measured tip-sample separations, the frequency noise is limited by detector noise at high offset frequencies. Detector noise increases $\propto f^2$ and is the dominant source of noise at offset frequencies of, for example, $f \geq 1$ Hz at $h = 1$ μm and $f \geq 80$ Hz at $h = 18$ nm. A software filter[6] has been used to suppress frequency fluctuations above $f \sim 100$ Hz in Fig. 4.

At large tip-sample separations ($h = 486$nm and $h = 1\mu$m) and intermediate offset frequencies (f near 1 Hz), the dominant source of cantilever noise is thermomechanical motion in the cantilever. We estimate a thermomechanical frequency noise of $P_{\delta f}^{\rm therm} = 1.4 \times 10^{-7}$ Hz^2/Hz from measured cantilever properties (Table I), temperature ($T = 4.2$ K), and cantilever amplitude (100 nm) using equations in Ref.6. This calculated thermomechanical frequency noise is in good agreement with the observed noise near $f \sim 1$Hz in the $h = 486$nm and $h = 1$ μm traces of Fig. 4.

As the cantilever is moved closer to the sample, surface-induced cantilever frequency noise becomes apparent at low offset frequencies. This noise is presumably due to interactions of residual charge on the tip with electric field gradient fluctuations in the sample.[1] At $h = 18$ nm, the power spectral density of cantilever frequency noise at low f is $\geq 10^7$ larger than the thermomechanical limit.

When using the cantilever near the surface in an electron spin resonance experiment, there is an optimal modulation frequency. This is because the surface-induced frequency noise decreases $\propto f$ while the detector noise increases $\propto f^2$. To measure the optimal modulation frequency, five 5 s transients of cantilever frequency were recorded and analyzed, as above, at a number of tip-sample separations. At each tip-sample separation, the optimal modulation frequency $f_{\rm mod}^{\rm opt}$ was deter-

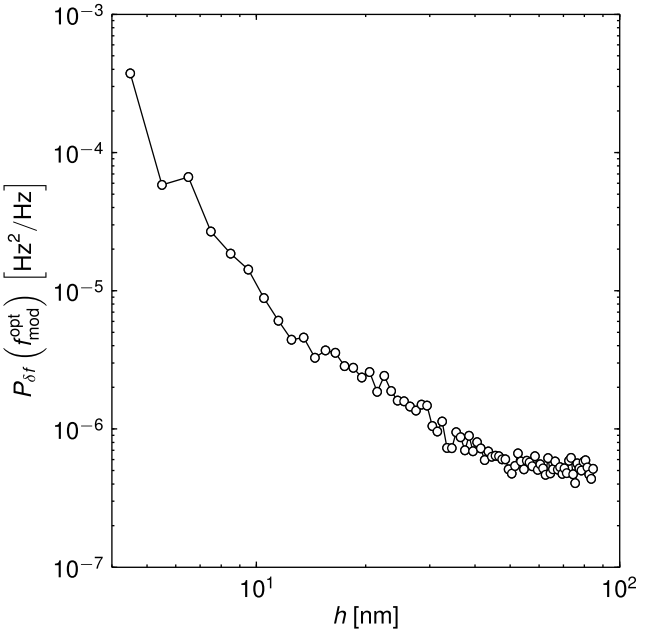

FIG. 5: Frequency noise at the optimal modulation frequency as a function of tip-sample separation.

mined by finding the minimum value of the power spectral density of cantilever frequency fluctuations. An eleven point moving average was used to smooth the observed cantilever frequency noise power spectrum in order to facilitate identifying the minimum in the spectrum.

The optimal modulation frequency ranged from 25 to 5 Hz for tip-sample separations ranging from 18 to 80 nm. A plot of the power spectral density of cantilever frequency fluctuations at $f = f_{\rm mod}^{\rm opt}$ is shown in Fig. 5. We can see that surface interactions are the dominant source of cantilever frequency noise at tip-sample separations below approximately $h = 70$ nm.

References

* Email:jam99@cornell.edu

[1] Yazdanian, S. M.; Hoepker, N.; Kuehn, S.; Loring, R. F.; Marohn, J. A. *Nano Lett.* **2009**, *9*, 2273 – 2279.
[2] Hutter, J.; Bechhoefer, J. *Rev. Sci. Instrum.* **1993**, *64*, 1868 – 1873.
[3] Marohn, J. A.; Fainchtein, R.; Smith, D. D. *Appl. Phys. Lett.* **1998**, *73*, 3778–3780.
[4] Stipe, B. C.; Mamin, H. J.; Stowe, T. D.; Kenny, T. W.; Rugar, D. *Phys. Rev. Lett.* **2001**, *86*, 2874 – 2877.
[5] Ng, T. N.; Jenkins, N. E.; Marohn, J. A. *IEEE Trans. Mag.* **2006**, *42*, 378.
[6] Yazdanian, S. M.; Marohn, J. A.; Loring, R. F. *J. Chem. Phys* **2008**, *128*, 224706.